Catalysis Letters Vol. 84, Nos. 1–2, November 2002 (©2002)

Synthesis and surface characteristics of zirconia and modified zirconia: Performance of CO hydrogenation

Daiping He, Yunjie Ding*, Hongmei Yin, Tao Wang, Hongyuan Luo and Can Li

Dalian Institute of Chemical Physics, The Chinese Academy of Sciences, Dalian 116023, China

Received 3 May 2002; accepted 8 August 2002

ZrO_2-A and ZrO_2-B catalysts were prepared by two different coprecipitation methods and their performance of CO hydrogenation was studied. The results indicated that ZrO_2 and Li-, Pd- and Mn-modified ZrO_2 catalysts exhibited good selectivity and high STY to higher alcohols. The surface characteristics of ZrO_2-A and ZrO_2-B samples were investigated by means of BET, NH_3–TPD, XRD and UV Raman technique. The tetragonal zirconia on the surface region of ZrO_2-A and Li–Pd–Mn/ZrO_2-A catalysts may be responsible for the high selectivity towards ethanol, while the monoclinic zirconia on the surface of ZrO_2-B and Li–Pd–Mn/ZrO_2-B catalysts may be crucial to the high isobutanol selectivity.

KEY WORDS: ZrO_2-based catalyst; CO hydrogenation; higher alcohol; surface characteristics of ZrO_2.

1. Introduction

Recent research interest in zirconia has greatly enhanced the prospects for applying this material as catalyst, catalyst support, ceramic, engineering gemstone, fuel cell, pigment, automotive gas sensor, etc. [1–6]. Its varied physical and chemical properties, including phase structure, reducing, oxidizing, and acidic and basic properties, make zirconia an attractive catalyst and catalyst support for a number of reactions [1,5,7–9]. For example, zirconia impregnated with sulfate ions has superacidic behavior and shows high activity for hydrocarbon isomerization and methanol conversion to hydrocarbons [10–13]. Meanwhile, other papers reported that zirconia itself can catalyze CO hydrogenation and produce isobutene with high selectivity at atmospheric pressure [14–18]. Studies of mixtures of zirconia for the synthesis of methanol and isobutanol can be found in a few cases. Recently Keim's group [19] reported a catalyst system based on zirconia mixed oxides which produced isobutanol very selectively during CO hydrogenation, and the space time yield of alcohols was up to 1059 g/L-h catalyst. The crude product contained methanol 56.8 wt%, isobutanol 30.2 wt%, and C_5+ alcohols 13.0 wt%. Typical research and motor octane numbers of the crude alcohol products are 108 and 91, respectively. Thus the studies on ZrO_2-based catalysts are significant.

In this work, the synthesis techniques of zirconia and modified zirconia and their performance of CO hydrogenation are studied. The effect of different synthesis techniques of zirconia on the surface characteristics and final reaction properties of ZrO_2-based catalysts is discussed.

2. Experimental

ZrO_2 catalysts were prepared from a solution of nitrate salt that was precipitated with NH_4OH to form a hydroxide gel in two different ways. ZrO_2-A was synthesized by slowly adding 14 mol/L aqueous ammonia (three times as much as $Zr(NO_3)_4$) to the solution of $Zr(NO_3)_4$ at 273 K under stirring. Before aging for 20 h, the pH valve of the solution was adjusted by 2 mol/L aqueous solution of NaOH until about 13.0. The precipitate thus obtained was washed thoroughly with deionic water until the pH of the filtrate was brought to 7.0 and then was dried at 383 K for 10 h. The dry precipitate was pelleted and calcined at 873 K for 4 h. Preparation of modified ZrO_2-A catalyst was conducted as follows: a solution of Li, Pd and Mn nitrates was concurrently impregnated on ZrO_2-A. The loadings of Li, Pd and Mn were 0.5 wt%, 1 wt% and 2 wt%, respectively. ZrO_2-B was prepared by adding an aqueous solution of $Zr(NO_3)_4$ slowly to an excess amount of 14 mol/L aqueous ammonia; the other procedures were the same as those of ZrO_2-A.

The catalyst was *in situ* reduced in a flow of H_2 before reaction. The temperature was raised 2 K/min from room temperature up to 723 K and then held constant for 1 h. The H_2 flow rate was 6 L/h at atmospheric pressure. Then the syngas ($H_2/CO = 2$, $CH_4 \approx 0.22\%$, $CO_2 \approx 1\%$) was fed into the catalyst

---

* To whom correspondence should be addressed.
E-mail: dyj@dicp.ac.cn

1011-372X/02/1100-0089/0 © 2002 Plenum Publishing Corporation

Table 1
Catalytic properties of ZrO_2-based catalysts[a].

Catalysts	Oxygenates STY[b] (g/kg-h)	Oxygenates distribution (mass%)					
		DME	C_1OH	C_2OH	C_3OH	i-C_4OH	Others[c]
ZrO_2-A	8.3	0	90.2	6.4	1.2	2.3	0
Li–Pd–Mn–ZrO_2-A	216.8	1.3	66.5	24.8	6.2	1.3	0
ZrO_2-B	33.9	5.4	87.1	0	0	7.5	0
Li–Pd–Mn–ZrO_2-B	135.9	0.7	73.7	0.7	0.7	22.2	0

[a] Reaction conditions: $T = 673\,K$; $P = 8.0\,MPa$; $SV = 15\,000\,h^{-1}$.
[b] Space-time yield.
[c] C_5^+ alcohols.

bed after cooling down to reaction temperature, and reacted for 4 h under $633 \sim 693\,K$, $6.0 \sim 8.0\,MPa$ and $GHSV = 10\,000 \sim 20\,000\,h^{-1}$ conditions. The loading of catalyst was 1 g (~0.8 ml) for each run. The reaction system consisted of a small fixed-bed tubular reactor with an external heating system, which was made of stainless with 450 mm length and 9 mm internal diameter. The effluent passed through a condenser filled with 100 ml of cold deionic water. The formed oxygenates were completely captured by dissolution into water in the condenser. The aqueous solution containing oxygenates was analyzed by off-line Varian CP-3800 gas chromatography with a PEG capillary column and FID as detector using 1-pentanol as an internal standard. The tail gas was analyzed by on-line Varian CP-3800 GC with a Porapak QS column and TCD as detector.

X-ray diffraction of zirconia prepared by different preparation methods was carried out on a Rigaku Rotaflex (RU-200B) power diffractometer equipped with a Cu target and an Ni filter. UV Raman spectra were recorded on a homemade UV Raman spectrograph, which has four main parts: a UV cw laser, a Spex 1877d triplemate spectrograph, a CCD detector, and an optical collection system. The 244-nm line from Innova 300 FRED was used as the excitation source. The laser power of the 244-nm line at the samples was below 2.0 mW. The textural properties of zirconia (specific surface area, pore volume, and mean pore radius) were determined from nitrogen adsorption–desorption isotherms at liquid nitrogen temperature by using a Micromeritics ASAP-2010 instrument. An NH_3–TPD test was carried out in a flow apparatus made by Micromeritics (Model Autochem 2910). The sample (0.2 g) was treated at its calcined temperature in helium flow for 1 h. After cooling to 423 K, the sample was saturated with NH_3. After this purging treatment, the sample was heated to 873 K at 10 k/min in a helium flow of $40\,cm^3/min$. The desorbed NH_3 was analyzed by an on-line gas chromatograph. The acidic amount on the surface of the catalysts was calculated by comparing the desorption amount of NH_3, which was determined by the areas of the desorption profiles.

3. Results and discussion

The activity and selectivity of CO hydrogenation over ZrO_2-based catalysts are shown in table 1. It was obvious that ZrO_2-A catalyst displayed good selectivity toward ethanol, while only dimethyl ether (DME), methanol and isobutanol were detected over ZrO_2-B catalyst. It was interesting to note that the space-time yield (STY) of ZrO_2-A increased dramatically from 8.3 up to 216.8 g/kg-h, and the selectivity of ethanol increased unexpectedly from 6.4 up to 24.8% when Li, Pd and Mn promoters were added into the ZrO_2-A catalyst. Similar promoting effects of Li, Pd and Mn promoters were observed in the case of the ZrO_2-B catalyst, but this catalyst exhibited good selectivity towards isobutanol. The selectivity of isobutanol was up to 22.2%.

Surface area, pore volume and mean pore radius are compiled in table 2. The BET surface area of the ZrO_2-A catalyst was $30.06\,m^2/g$, while that of the ZrO_2-B catalyst was $51.59\,m^2/g$. The mean pore radius and pore volume of ZrO_2-A were larger than those of ZrO_2-B. Two possible processes were responsible for the changes occurring in the pore structure and surface area: crystallite growth and the accompanying phase transformation.

Figure 1 exhibits the X-ray diffraction patterns of ZrO_2-A and ZrO_2-B samples studied in this work. The diffraction peaks of the tetragonal phase were predominant, and almost no peaks of the monoclinic phase were found in the ZrO_2-A and ZrO_2-B samples. It was found that the crystallinity of ZrO_2-B was better than that of ZrO_2-A.

Table 2
Textural properties of ZrO_2-A and ZrO_2-B catalysts[a].

Catalysts	S_{BET} (m^2/g)	V_p (mL/g)	R_p (Å)
ZrO_2-A	30.06	0.124	165.09
ZrO_2-B	51.59	0.092	70.56

[a] Specific surface area (S_{BET}), pore volume (V_p), and mean pore radius (R_p).

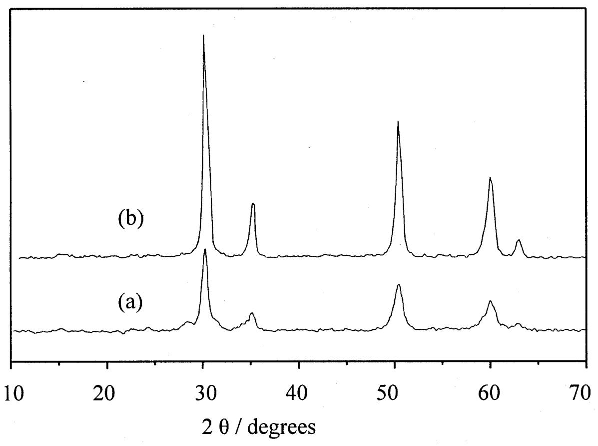

Figure 1. X-ray diffraction patterns of (a) ZrO_2-A and (b) ZrO_2-B.

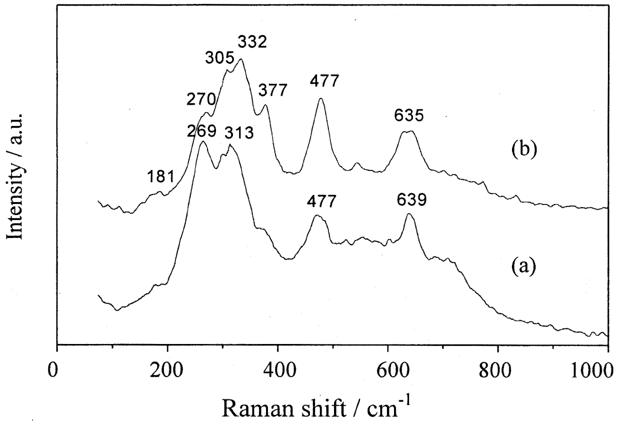

Figure 3. UV–Raman Spectra of (a) ZrO_2-A and (b) ZrO_2-B.

Jackson *et al.* studied the surface characteristics required for iso-synthesis over zirconia [20]. For the two iso-synthesis chain growth reactions (condensation and CO insertion), Lewis acidic sites were found to enhance the condensation reaction. The CO insertion reaction was enhanced by basic sites that were activated by high-temperature treatment. The selectivity of the iso-synthesis reaction was caused by a balance between the strength and quantity of acidic and basic sites on zirconia.

Figure 2 displays NH_3–TPD profiles of the ZrO_2-A and ZrO_2-B samples. It was found that there were two kinds of desorption peaks of ammonia at 512 and 650 K on the surface of the ZrO_2-B catalyst, while only one NH_3–TPD peak at 624 K on the surface of the ZrO_2-A catalyst. It is worth noting that the total quantity of NH_3 desorption was almost the same, implying little difference in the strength and number of acidic sites on the surface of the ZrO_2-A and ZrO_2-B catalysts. Therefore, it is difficult for the surface acidic and basic properties of zirconia to be responsible for the variation in activity and selectivity of CO hydrogenation over the ZrO_2-A and ZrO_2-B catalysts.

Ultraviolet Raman spectroscopy (UVRS) is a powerful tool for the study of surface characteristics of catalysts and other solids [21]. Figure 3 shows the UV Raman spectra of ZrO_2-A and ZrO_2-B samples. The UV Raman spectrum of ZrO_2-A gives strong bands at 269, 313, 477 and 639 cm^{-1}. These features are readily attributed to the tetragonal and monoclinic zirconia, but the tetragonal zirconia is dominant, while the typical Raman bands at 181, 270, 305, 332, 377, 477 and 635 cm^{-1}, attributed to monoclinic zirconia [21], can be observed in the ZrO_2-B catalyst. Almost no peaks attributed to tetragonal ZrO_2 were detected in this sample. It is well known that UV Raman spectroscopy is more sensitive to the surface region of catalysts and other solids [22–24], especially for the surface region of zirconia because zirconia shows a strong absorbance in the UV region [21]. It is obvious, from the combination of XRD patterns and UV Raman spectra, that there is only tetragonal zirconia in the bulk and the surface region of ZrO_2-A but tetragonal zirconia in the bulk and monoclinic zirconia on the surface of ZrO_2-B.

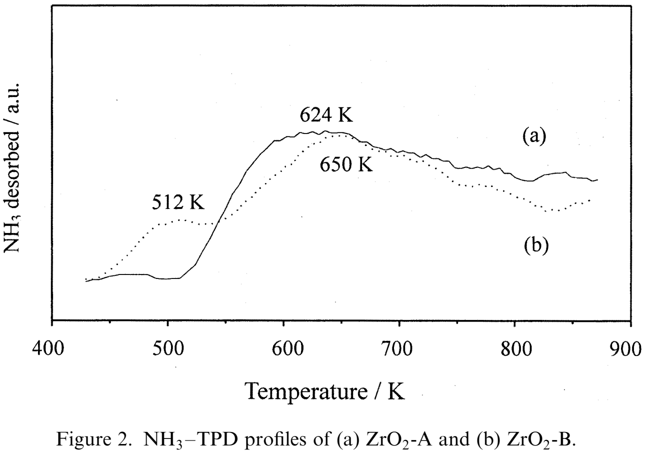

Figure 2. NH_3–TPD profiles of (a) ZrO_2-A and (b) ZrO_2-B.

All the observations allow us to propose that the tetragonal zirconia on the surface region of the ZrO_2-A and Li–Pd–Mn/ZrO_2-A catalysts may be responsible for the high selectivity toward ethanol, while the monoclinic zirconia on the surface of the ZrO_2-B and Li–Pd–Mn/ZrO_2-B catalysts may be crucial to the high isobutanol selectivity.

In order to ensure the performance of the two kinds of zirconia and modified zirconia catalysts, the optimum conditional experiments, such as reaction temperature, pressure and space velocity, were carried out. At conditions of 8.0 MPa and 15 000 h^{-1}, the effect of reaction temperature in the range 633 ∼ 693 K on the product distribution over ZrO_2-based catalysts is shown in table 3. It is apparent that the selectivity of ethanol over Li–Pd–Mn/ZrO_2-A catalyst or that of isobutanol over Li–Pd–Mn/ZrO_2-B catalyst in alcohols increased gradually with increasing temperature, the space-time yield (STY) of ethanol over the Li–Pd–Mn/ZrO_2-A catalyst passed through a maximum at 673 K, while STY of isobutanol over the Li–Pd–Mn/ZrO_2-B

Table 3
Effect of temperature on catalytic performance ZrO_2-based catalysts[a].

Catalysts	T (K)	Oxygenate STY[b] (g/kg-h)	Oxygenate distribution (mass%)					
			DME	C_1OH	C_2OH	C_3OH	i-C_4OH	Others[c]
Li–Pd–Mn–ZrO_2-A	633	219.4	0.7	88.2	9.2	1.5	0.4	0
	653	261.3	0.7	79.9	14.7	3.8	1.0	0
	673	216.8	1.3	66.5	24.8	6.2	1.3	0
	693	167.5	2.1	62.7	26.3	7.4	1.5	0
Li–Pd–Mn–ZrO_2-B	633	205.3	0.5	86.8	2.2	1.1	9.0	0
	653	195.1	0.5	80.2	0.8	0.9	16.2	1.5
	673	135.9	0.7	73.7	0.7	0.7	22.2	0

[a] Reaction conditions: SV = 15 000 h^{-1}, $P = 8.0$ MPa.
[b] Space-time yield.
[c] C_5^+ alcohols.

Table 4
Effect of pressure on catalytic performance ZrO_2-based catalysts[a].

Catalysts	P (MPa)	Oxygenate STY[b] (g/kg-h)	Oxygenate distribution (mass%)					
			DME	C_1OH	C_2OH	C_3OH	i-C_4OH	Others[c]
Li–Pd–Mn–ZrO_2-A	6.0	126.9	0.5	85.6	10.2	3.1	0.6	0
	8.0	261.3	0.7	79.9	14.7	3.8	1.0	0
Li–Pd–Mn–ZrO_2-B	6.0	117.6	0.9	84.4	0.5	0.7	12.9	0.6
	8.0	195.1	0.5	80.2	0.8	0.9	16.2	1.5

[a] Reaction conditions: SV = 15 000 h^{-1}, $T = 653$ K.
[b] Space-time yield.
[c] C_5^+ alcohols.

catalyst passed through a maximum at 653 K. It is concluded that 673 K is the optimum temperature for ethanol synthesis over the Li–Pd–Mn/ZrO_2-A catalyst, while 653 K is the optimum temperature for isobutanol synthesis over the Li–Pd–Mn/ZrO_2-B catalyst.

The effect of pressure on catalytic performance of ZrO_2-based catalysts is shown in table 4. The STY and selectivity of ethanol over the Li–Pd–Mn/ZrO_2-A catalyst or those of isobutanol over the Li–Pd–Mn/ZrO_2-B catalyst increased as the pressure was increased. Therefore, high pressure is more favorable for ethanol and isobutanol synthesis.

Table 5 shows the effect of gas hourly space velocity (GHSV); the STY and selectivity of ethanol over Li–Pd–Mn/ZrO_2-A catalyst or those of isobutanol over Li–Pd–Mn/ZrO_2-B catalyst increased with increasing

Table 5
Effect of GHSV on catalytic performance ZrO_2-based catalysts[a].

Catalysts	SV (h^{-1})	Oxygenate STY[b] (g/kg-h)	Oxygenate distribution (mass%)					
			DME	C_1OH	C_2OH	C_3OH	i-C_4OH	Others[c]
Li–Pd–Mn–ZrO_2-A	10 000	143.6	0.6	82.4	11.5	4.7	0.9	0
	15 000	261.3	0.7	79.9	14.7	3.8	1.0	0
	17 500	288.1	0.2	79.3	16.6	3.1	0.5	0.3
	20 000	295.9	0.2	78.7	17.1	3.0	0.8	0.2
Li–Pd–Mn–ZrO_2-B	10 000	129.5	2.0	85.3	0.9	0.6	10.5	0.5
	15 000	195.1	0.5	80.2	0.8	0.9	16.2	1.5
	17 500	215.4	0.7	80.1	0.9	0.7	16.4	1.2
	20 000	253.2	0.4	79.7	1.1	0.8	16.7	1.3

[a] Reaction conditions: $T = 653$ K, $P = 8.0$ MPA.
[b] Space-time yield.
[c] C_5^+ alcohols.

GHSV, indicating the higher alcohols are formed *via* primary processes, which is in accordance with the classical rule for higher alcohol synthesis [25].

4. Conclusions

The surface characteristics, such as surface phases, on zirconia and modified zirconia catalysts may play an important role in the performance (especially for the selectivity of higher alcohols) of their CO hydrogenation. The different selectivity for ZrO_2-based catalysts, leading to ethanol or isobutanol, depends greatly on the surface phases of ZrO_2 and Li-, Pd- and Mn-modified ZrO_2 catalysts prepared by different techniques. The tetragonal zirconia on the surface region of ZrO_2-A and Li–Pd–Mn/ZrO_2-A catalysts may be responsible for the high selectivity toward ethanol, while the monoclinic zirconia on the surface of ZrO_2-B and Li–Pd–Mn/ZrO_2-B catalysts may be crucial to the high isobutanol selectivity. For the Li–Pd–Mn/ZrO_2-A catalyst, 673 K, higher space velocity and pressure are the optimum reaction conditions for ethanol synthesis from syngas. At 8.0 MPa, 673 K and 15 000 h^{-1}, ethanol selectivity reached 24.8%. For the Li–Pd–Mn/ZrO_2-B catalyst, its optimum temperature was 653 K. Higher space velocity and pressure were more favorable for isobutanol synthesis. At 8.0 MPa, 653 K and 15 000 h^{-1}, isobutanol selectivity was increased up to 16.2%.

Acknowledgment

This work was financially supported by the Innovation Funding of the Dalian Institute of Chemical Physics, The Chinese Academy of Sciences.

References

[1] R. Srinivasan and B.H. Davis, Catal. Lett. 14 (1992) 165.
[2] G. Stefanic, S. Music, B. Grzeta, S. Popovic and A. Sekulic, J. Phys. Chem. Solids 59 (1998) 879.
[3] B. Xia, L.Y. Duan and Y.CH. Xie, J. Am. Ceram. Soc. 83 (2000) 1077.
[4] S.C. Su and A.T. Bell, J. Phys. Chem. B 102 (1998) 7000.
[5] Z. Dang, B.G. Anderson, Y. Amenomiya and B.A. Morrow, J. Phys. Chem. 99 (1995) 14437.
[6] J.M. Miller and L.J. Lakshmi, J. Phys. Chem. B 102 (1995) 6465.
[7] K. Tanabe, Mater. Chem. Phys. 13 (1985) 347.
[8] R. Srinivasan, D. Taulbee and B.H. Davis, Catal. Lett. 9 (1991) 1.
[9] K. Tanabe, M. Misono, Y. Ono and H. Hattori, Stud. Surf. Sci. Catal. 51 (1989) 1.
[10] M. Hino, S. Kobayashi and K. Arata, J. Am. Chem. Soc. 101 (1979) 6439.
[11] B.H. Davis, R.A. Keogh and R. Srinivasan, Catal. Today 20 (1994) 219.
[12] C. Morterra, V. Bolis, G. Cerrato and G. Magnacca, Surf. Sci. 304 (1994) 1206.
[13] H. Makoto and A. Kazushi, Appl. Catal. 18 (1985) 401.
[14] H. Maehashi, K. Maruya, K. Domen, K. Aika and T. Onishi, Chem. Lett. 149 (1984) 747.
[15] K. Maruya, T. Fujisawa, A. Takasawa, K. Domen and T. Onishi, Bull. Chem. Soc. Jpn. 62 (1989) 11.
[16] K. Maruya, J. Japan. Petroleum Institute 37 (1994) 246.
[17] K. Maruya, Catal. Lett. 24 (1994) 349.
[18] M.Y. He and J.G. Ekerdt, J. Catal. 87 (1984) 238.
[19] M. Roper, W. Keim, J. Seibring and G. Kolle, DE 3524317 (1987).
[20] N.B. Jackson and J.G. Ekerdt, J. Catal. 57 (1990) 127.
[21] M.J. Li, Z.C. Feng, G. Xiong, P.L. Ying, Q. Xin and C. Li, J. Phys. Chem. B 105 (2001) 8107.
[22] P.C. Stair and C. Li, J. Vac. Sci. Technol. A 15 (1997) 1679.
[23] C. Li and P.C. Stair, Stud. Surf. Sci. Catal. 105 (1997) 599.
[24] C. Li and P.C. Stair, Catal. Lett. 36 (1996) 119.
[25] Y.Q. Niu, Z.H. Chen, X.L. Liu, Y. Li and L.H. Bo, J. Fuel Chem. Technol. (in Chinese) 16 (1988) 82.